We are IntechOpen, the world's leading publisher of Open Access books Built by scientists, for scientists

4,800
Open access books available

122,000
International authors and editors

135M
Downloads

Our authors are among the

154
Countries delivered to

TOP 1%
most cited scientists

12.2%
Contributors from top 500 universities

CLARIVATE ANALYTICS BOOK CITATION INDEX INDEXED

WEB OF SCIENCE™

Selection of our books indexed in the Book Citation Index in Web of Science™ Core Collection (BKCI)

Interested in publishing with us?
Contact book.department@intechopen.com

Numbers displayed above are based on latest data collected.
For more information visit www.intechopen.com

2

PVA / Montmorillonite Nanocomposites: Development and Properties

Andreas A. Sapalidis, Fotios K. Katsaros and Nick K. Kanellopoulos
N.C.S.R. Demokritos, Institute of Physical Chemistry, Greece

1. Introduction

Polymers are hardly used in their pure form in applications; they are often filled with additives. The modification of polymers, through the incorporation of additives in the micrometer range, e.g. calcium carbonate, glass beads and talc, yields, with few exceptions, multiphase systems containing the additive embedded in a continuous polymeric matrix. The additives can either improve their process ability (lubricants, antioxidants and stabilizers), or modify the modulus and the strength (carbon black, silica beads and fibers, clay, mica), the appearance (pigments and surfactants), the conductivity (carbon black and carbon nanotubes), the transport properties, the moisture content, the flammability or simply reduce their cost (Alexandre & Dubois, 2000), (Fischer, 2003), (Lagaly, 1999), (Giannelis, 1996).

On the other hand, polymer nanocomposites represent a class of material alternative to conventional filled polymers. In this type of materials, nanofillers (having at least one dimension in nanoscale range) are finely dispersed in polymer matrix offering remarkable improvement in performance properties of the polymer, including high moduli (LeBaron et al., 1999), (Giannelis et al., 1999), (Vaia et al., 1999) increased strength (Giannelis, 1998) and heat resistance (Gilman, 1999), improved gas barriers properties (Xu et al., 2001), (Sinha-Ray et al., 2002) and fire redundancy (Gilman et al., 2000), (Morgan, 2006) etc.

There are four major parameters affecting the final properties of the nanocomposites, namely:

i. the filler aspect ratio,
ii. the filler dispersion,
iii. the filler alignment and orientation and
iv. the polymer-polymer and polymer-filler interfacial interactions.

The control and the optimization of the above-mentioned structural factors are expected to enable the development of nanocomposites with predefined and superior properties. Interfaces can greatly affect the properties of a composite. The large surface area of the filler can be either advantageous or disadvantageous, depending on the type of property. For example, it may result in a composite of low strength (in spite of the possibly high strength within a single unit of the nanofiller, e.g., within a single nanofiber) due to the mechanical weakness of the interface. It may also result in a composite of high electrical resistivity due to the electrical resistance associated with the interface.

Numerous potential nanosized fillers, with high aspect ratio, have been utilized for the preparation of high efficient nanocomposites. Amongst them, clay and layered silicates have been more widely investigated, probably due to their availability and their low cost. Furthermore, their well-studied intercalation chemistry offers additional advantages for their application in nanocomposite technology.

Polymer nanocomposites are two-phase materials, in which the polymers are reinforced by nanoscale fillers. One of the most extensively used filler material is the smectite class of aluminum silicate clays, of which the most common representative is montmorillonite (MMT). MMT has been employed in many Polymer/Layered Silicates (PLS) nanocomposite systems because it has a potentially high-aspect ratio and high-surface area that could lead to materials, which could possibly exhibit great property enhancements. In addition, it is environmentally friendly, naturally occurring, and readily available in large quantities.

However, since the layered silicates in their pristine state are hydrophilic, the nanolayers are not easily dispersed in most polymers and tend to form agglomerates. Dispersion of the inorganic platelets into discrete monolayers is further hindered by the intrinsic incompatibility of hydrophilic layered silicates and hydrophobic engineering plastics. Therefore, in most cases, layered silicates must initially be organically modified to produce well-organized nanocomposites. On the other hand, MMT is capable of forming stable suspensions in water, while its hydrophilic character also promotes the dispersion of these inorganic crystalline layers in water soluble polymers, such as poly(vinyl alcohol), poly(ethylene oxide) etc.

Poly(vinyl alcohol) (PVA) is a water soluble polymer extensively used in paper coating, textile sizing, and flexible water soluble packaging films. However, the insufficient mechanical properties and the poor resistance in solvents have limited its applicability in industrial processes. Development of PVA-based nano-composites has been an emerging method to improve PVA's properties. Thus, PVA/layered silicate nanocomposite materials with improved mechanical, thermal, and permeability properties may offer a viable alternative for these applications to heat treatments (that may cause polymer degradation) or conventionally filled PVA materials, which are optically opaque.

This chapter highlights the major developments in the preparation of PVA/MMT nanocomposites during the last decades. Furthermore, the authors, based on polymer-polymer and polymer-clay interactions, describe an effective way for the preparation of well-dispersed nanocomposites with improved properties. The obtained nanocomposites were characterised by a variety of techniques, including XRD, TEM, AFM, DCS, TGA, mechanical strength, oxygen permeability and water sorption. The developed films, due to the favorable polymer-particle interactions, revealed excellent dispersion of the clay particles in the polymer matrix and improved properties.

2. Structure of polymer and layered silicates

2.1 Structure of MMT

The commonly used layered silicates for the preparation of polymer/layered silicate (PLS) nanocomposites belong to the same general family of 2:1 layered- or phyllosilicates (Alexandre & Dubois, 2000). Their unit lamellar crystal is composed of two crystal sheets of silica tetrahedron combined with one crystal sheet of alumina octahedron between them (Ray & Bousmina, 2006). The layer thickness is about 1 nm, while the lateral dimensions of these layers may range from a few nanometers to several microns or several hundreds of

microns, depending on the particular layered silicate, the source of the clay and the method of preparation. Therefore, the aspect ratio i.e. the length to thickness ratio of these layers is particularly high, reaching values even greater than 1000 (McNally et al., 2003), (Pavlidou & Papaspyrides, 2008).

The layers of the silicates can easily be self-organized to form stacks with a regular van der Walls gap in between them, called the interlayer or the gallery. Isomorphic substitution within the layers (for example, Al^{+3} replaced by Mg^{+2} or by Fe^{+2}, or Mg^{+2} replaced by Li^{+}) generates negative charges that are counterbalanced by alkali or alkaline earth cations – mainly sodium and calcium ions, existing hydrated in the interlayer. As the forces that hold the stacks together are relatively weak, small molecules including water, solvents, and monomer as well as polymer, can enter into these galleries, causing the lattice to expand (Giannelis, 1996), (Nguyen & Baird, 2006). A characteristic value of *d*-spacing is reported for each type of layered silicate. The *d*-spacing is the repeat unit in the crystalline structure including the 1 nm thick platelet and the spacing in between the platelet sheets (Brindley, 1984).

The layered silicates characterized by a moderate surface charge known as the cation exchange capacity (CEC), which is generally expressed as mequiv/100 g. The charge is not locally constant, but varies from layer to layer, and must be considered as an average value over the whole crystal. In the case of tetrahedrally-substituted layered silicates, the negative charge is located on the surface of silicate layers, and hence, the polymer matrices can interact more readily with these than with octahedrally-substituted material (Ray & Bousmina, 2006). The advantages of the layered silicates that are generally considered for PLS-nanocomposites preparation are mainly related to their ability to form exfoliated structures (individual platelets) and to the straightforward and effective functionlisation of their surface. The exfoliated/intercalated structures provide high aspect ratios and high-surface areas, leading to nanocomposites with improved final properties. On the other hand, the surface chemistry of the layers can be adjusted through ion exchange reactions with organic and inorganic cations.

Montmorillonite, which is the best-known member of a group of clay minerals, called "smectites" or "smectite clays", is the most widely used layered silicate for the preparation of nanocomposites. Montmorillonite has a 2:1 structure, which allows sharing of the oxygen between Al and Si. Additionally, there are hydroxyl groups at the edges of each clay platelet. The structure of montmorillonite is shown in Figure 1, while its general formula is (Pinnavaia & Beall, 2000):

$$(Na,Ca)_{0.33}(Al,Mg)_2(Si_4O_{10})(OH)_2 \cdot nH_2O \quad (1)$$

Montmorillonite is a hydrophilic, inorganic material, which usually contains hydrated Na+ or K^+ ions (Krishnamoorti et al., 1996). Therefore, in this pristine state, layered silicates are only miscible with hydrophilic polymers, such as poly(ethylene oxide) (PEO) (Aranda & Ruiz-Hitzky, 1992) or poly(vinyl alcohol) (PVA) (Strawhecker & Manias, 2000), (Yu et al., 2003). To render layered silicates miscible with hydrophobic polymer matrices, one must convert the normally hydrophilic silicate surface to an organophilic one, making the intercalation of polymer chains into inorganic galleries more effective.

Generally, this can be done by ion-exchange reactions with cationic surfactants including primary, secondary, tertiary, and quaternary alkylammonium or alkylphosphonium cations. This, results in expansion between the clay galleries, due to the larger molecules inserted between the layers. The reaction also changes the clay from hydrophilic to hydrophobic,

making it more compatible with the organic matrix. Additionally, the alkylammonium or alkylphosphonium cations can provide functional groups that can react with the polymer matrix, or in some cases initiate the polymerization of monomers to improve the adhesion between the inorganic and the polymer matrix (Messersmith & Giannelis, 1995), (Gilman et al., 2000).

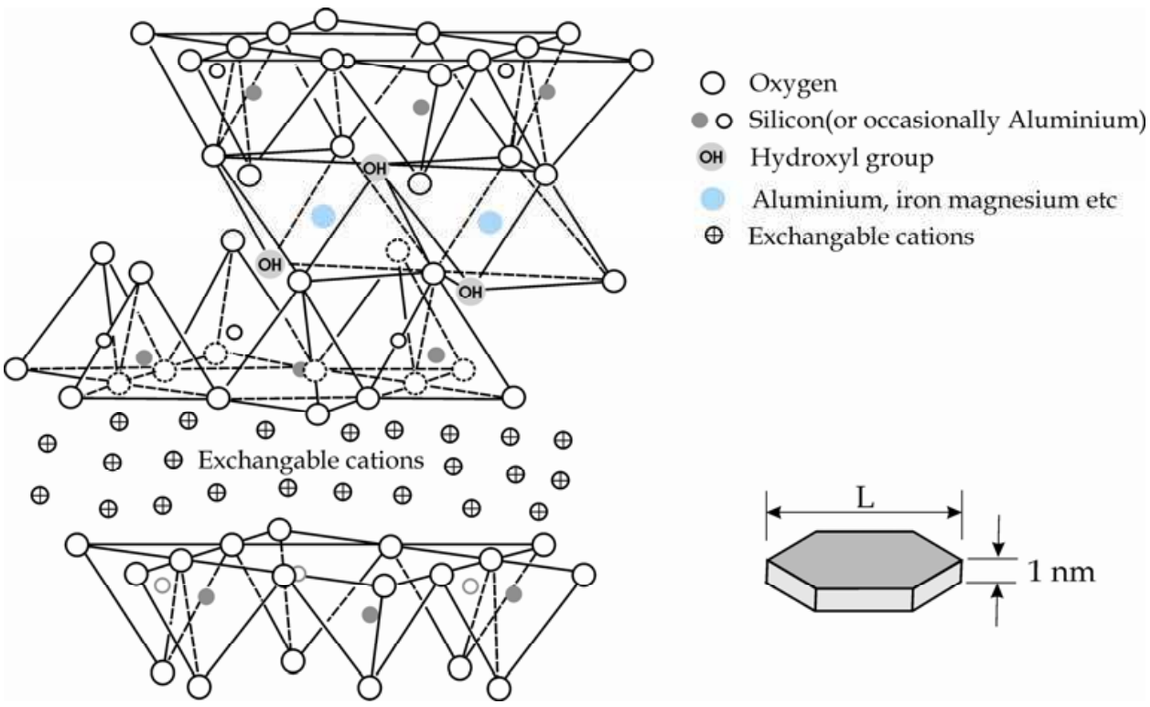

Fig. 1. Structure of 2:1 layered silicate showing two tetrahedral sheets of silicon oxide fused to an octahedral sheet of aluminum hydroxide and Platelet structure

2.2 Polyvinyl alcohol (PVA)

PVA is the most widely produced water soluble polymer today. It has been available since 1924, when its synthesis via the saponification of poly-(vinyl acetate) was first described by Herrmann and Haehnel (Herrmann & Haehnel, 1924). PVA is currently produced from the parent homopolymer poly(vinyl acetate) (PVAc) via hydrolysis (methanolysis) (Hay & Lyon, 1967). Its application has mainly been focused on fibre industry. Recently, it has received much attention in non-fibre applications specifically in pharmaceutical, biomedical and biochemical applications, due to its attractive characteristics, such as biocompatibility, biodegradability, and water-solubility. PVA has been also used for membranes (Chuang et al., 2000), drug delivery system (Brazel & Peppas, 1999), and artificial biomedical devices (Kobayashi et al., 2003).

However, the undesirable properties of PVA, including the poor solvent resistance and anti-ageing behaviour, the insufficient strength and the low heat stability, have restricted its further applications. Thus, the preparation of PVA-based conventional (Sapalidis et al., 2007) as well as nano-composites (Chang et al., 2003), (Yu et al., 2003), (Podsiadlo et al., 2007) in order to improve the mechanical, the thermal, and the gas barrier properties have attracted several research studies.

2.3 Nanocomposite structure

In general, the degree of dispersion of the clay platelets into the polymer matrix determines the structure and the final properties of the nanocomposites. Depending on the nature of the components used (layered silicate, organic cation and polymer matrix) and the method of preparation, three main types of composites may be obtained, when layered clay is associated with a polymer (Figure 2):

a. *Non mixing composites:* In this case, the interactions between the clay particles and the polymer are very weak and thus, the polymers cannot enter into clay galleries. A phase separated composite is formed with relatively poor mechanical properties (Alexandre & Dubois 2000).
b. *Intercalated structures*: in which the polymeric chains are intercalated between the silicate layers resulting in a well ordered multilayer morphology, built up with alternating polymeric and inorganic layers. Intercalation results a separation of about 2-3 nm between the layers, which is independent of the clay to polymer ratio (Yeh & Chang, 2008). The properties of this type of nanocomposites resemble those of ceramic materials.
c. *Exfoliated or delaminated structures*: in which the clay layers are well separated from one another and individually dispersed in the continuous polymer matrix (Giannelis, 1996). In this case, the distance between two platelets may be in the range of 5-10 nm or even more (Dennis et al., 2001). In such systems, the polymer–clay interactions are maximised leading to significant changes in mechanical and physical properties. It is generally accepted that exfoliated systems exhibit better mechanical properties than intercalated ones (Varlot et al., 2001), (Chin et al., 2001).

2.4 Techniques used for the characterization of nanocomposites

Since the properties of the nanocomposites are defined by the dispersion of the inorganic nanoplatelets into the polymer, one needs to know the degree of exfoliation /intercalation of a particular sample and compare it to other samples. A number of methods have been reported in the literature for this purpose (Krishnamoorti et al., 1996), (Morgan & Gilman, 2003), (Van der Hart et al., 2001). Generally, the state of dispersion and exfoliation of

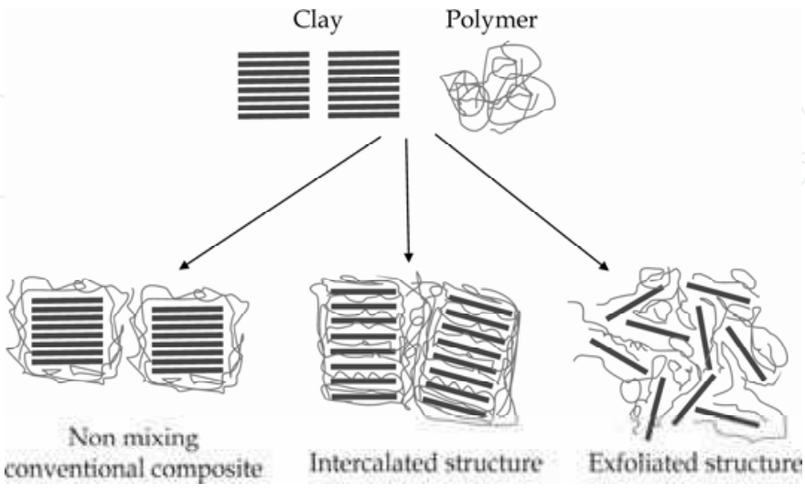

Fig. 2. Schematic representation of the three types of composite structures depending on polymer –clay interactions

nanoparticles has typically been studied using X-ray diffraction (XRD) analysis and transmission electron microscopy (TEM) observations. Due to its easiness and availability, XRD is most commonly used to probe the nanocomposite structure (Giannelis et al., 1999), (Biswas & Ray, 2001), (Ray & Okamoto, 2003). The nanocomposite structure, namely, intercalated or exfoliated, may be identified by monitoring the position, shape, and intensity of the basal reflections, from the distributed silicate layers. For example, in an exfoliated nanocomposite, the extensive layer separation associated with the delamination of the original silicate layers in the polymer matrix results in the eventual disappearance of any coherent X-ray diffraction from the distributed silicate layers. On the other hand, for intercalated nanocomposites, the finite layer expansion associated with the polymer intercalation results in the appearance of a new basal reflection corresponding to the larger gallery height. Additionally, in some cases, XRD is employed to study the kinetics of the polymer melt intercalation (Vaia et al., 1996).

Although XRD offers a convenient method to determine the interlayer spacing of the silicate layers in the original layered silicates and in the intercalated nanocomposites (within 1-4 nm), little can be said about the spatial distribution of the silicate layers or the structural homogeneity of the nanocomposites. In addition, some layered silicates do not exhibit well-defined basal reflections, consisting that way difficult the determination of the intensity pattern and the shape of the relative peaks (Zanetti et al., 2000).

Therefore, conclusions concerning the mechanism of nanocomposites formation and their structure based solely on XRD patterns are only tentative. On the other hand, TEM allows a qualitative understanding of the internal structure, spatial distribution and dispersion of the nanoparticles within the polymer matrix, and views of the defect structure through direct visualization. However, special care must be exercised to guarantee a representative cross section of the sample.

Both techniques are essential tools for evaluating nanocomposite structure (Morgan & Gilman, 2003). However, when layer spacing exceeds 6-7 nm in intercalated nanocomposites or when the layers become relatively disordered in exfoliated nanocomposites, XRD features weaken to the point of not being useful.

To this end, numerous advanced techniques can be employed for the characterization of the nanocomposites. Recent simultaneous small angle X-ray scattering (SAXS) and XRD studies yielded quantitative characterization of nanostructure and crystallite structure in some nanocomposites (Bafna et al., 2003). In addition, neutron membrane diffraction technique can reveal information about both the dispersion and the orientation of the inorganic layers in the polymer matrix (Katsaros et al., 2009).

In contrast to the conventional electron microscopy, Atomic Force Microscopy (AFM) represents an effective alternative method to study the dispersion of the nanofillers without any limitations regarding the sample preparation, the contrast and the resolution. Atomic force microscopy, although increasingly being used in polymer structure characterization (Magonov & Reneker, 1997), (Magonov, 2000), surprisingly has not been widely used to investigate the layered silicate nanocomposite systems (Clement et al., 2001), (Yalcin & Cakmak, 2004), (Maiti & Bhowmick, 2006). The development of this technique has helped to image surface topography on nanoscale. Thus, apart from the investigation of clay dispersion AFM can provide information about surface topography of the samples. In addition, AFM can also measure fundamental properties of sample surfaces, e.g., local adhesive or elastic properties on nanoscale (Malwitz et al., 2004), (McNally et al., 2003), (Jiang et al., 2005).

2.5 PVA/MMT nanocomposites

Poly(vinyl alcohol) – clay nanocomposite materials have widely been studied in the past. Greenland (Greenland, 1963) reported the first fabrication of PVA/MMT composites by a solvent casting method, using water as a co-solvent. Ogata and coworkers (Ogata et al. 1997) applied the same technique for the production of PVA/MMT composites. Furthermore, Strawhecker and Manias (Strawhecker & Manias, 2000) have also developed PVA/MMT nanocomposites films with improved properties, by means of solvent casting method using low viscosity, fully hydrolyzed atactic PVA. The obtained nanocomposite films (clay content up to 5 wt %) exhibited both intercalated and exfoliated regions.

Recently, Chang and coworkers (Chang et al., 2003) reported the preparation of PVA-based nanocomposites with three different types of clays, namely pristine MMT and two different types of organically modified MMT (Dodecylamine and 12- aminolauric modified montmorillonite). They applied the same solvent casting method, but used also N,N-dimethylacetamide (DMAc) as co-solvent in addition to water. XRD patterns and TEM observations of their nanocomposites revealed the formation of exfoliated nanocomposites when pristine clays were used for the fabrication of nanocomposites. On the other hand, intercalated nanocomposites were produced with organo- modified clays. This implies that the hydrophilic character of clay promotes the effective dispersion of the inorganic crystalline layers in water-soluble polymers.

Based on in-situ intercalative polymerisation, Yu et al. (Yu et al., 2003) reported the synthesis of a series of PVA/MMT nanocomposites, using AIBN as initiator. In the first step of their preparation, the vinyl acetate monomers were intercalated into the organically modified clay galleries. Free radical polymerisation was followed in the subsequent step. The final PVA/MMT nanocomposites were obtained after hydrolysis of the vinyl acetate groups. The structural characterization of the developed materials confirmed the formation of mixed intercalated/exfoliated regions.

More recently a highly ordered Poly(vinyl alcohol) / montmorillonite nanocomposites were produced by the layer by layer (LBL) process (Podsiadlo et al., 2007). The LBL process is based on sequential adsorption of nanometer-thick monolayers of oppositely charged compounds (such as polyelectrolytes, charged nanoparticles, and biological macromolecules) to form a multilayered structure with nanometer-level control over the architecture. The obtained nanocomposites exhibited superior mechanical properties without significant reduced in optical transparency.

At equilibrium, the nanocomposite structure predicted from thermodynamics corresponds to an intercalated periodic nanocomposite with *d*-spacing around 1.8 nm, which is expected to be independent of the polymer-to-silicate ratio (Lee et al., 1998). However, thermodynamics can only predict the equilibrium structure. On the other hand, the nanocomposite structure is mainly determined by kinetic factors. In water solutions, PVA and MMT layers remain in colloidal suspension. During slowly drying, the silicate layers remain distributed and embedded in the polymer gel. Additional drying removes all of the solvent, and although the thermodynamics would predict the MMT layers to re-aggregate, the slow polymer dynamics entrap some of the layers and keep them separated. Therefore, the platelets remain dispersed in the polymer matrix. Obviously, the kinetic constraints imposed by the polymer become less important as the polymer-to-silicate fraction decreases, and consequently, for higher amounts of MMT, intercalated structures are formed. For these periodic structures, the variation of the d-spacing with wt% of MMT reflects the different polymer-silicate weight ratios, and upon increasing the amount of MMT the intercalated d-spacing converges to the equilibrium separation of 1.8 nm (Ray & Bousmina, 2006)

The structures obtained during the addition of clay particles in a polymer solution are determined by the polymer-polymer and polymer-clay interactions (Lim et al. 2001). These interactions enable the chains to receive certain conformations and to build structures around the inorganic layers. Depending on the nature of the adhesion (strong or weak), these arrangements lead to the formation of larger assemblies like structured intercalated regions. Theoretical and experimental results demonstrate that the adhesive role of a polar polymer between hydrophilic clay layers, the so called "glue effect", tends to strongly prohibit complete dissociation of the layered structure of the clay, resulting in an ordered intercalated state (Lee et al., 2006).

In pure PVA, the hydrogen bonds are the dominant interaction responsible for both structure and molecular dynamics. As a consequence of these bonding interactions, water is capable to destroy inter- and intra- chain hydroxyl bonds, affecting PVA's crystalline regions and acting as a plasticizer, increasing the free-volume of the amorphous phase (Hodge et al. 1996). On the other hand, in PVA/MMT nanocomposites, the interactions of the surface of the clay with the polymer can be attributed to the formation of hydrogen bonds between the PVA hydroxyl groups and the negatively charged clay surface (Grunlan et al., 2004), (Hernández et al., 2008).

Thus, in previous studies, the authors trying to maximise the polymer-clay interactions, utilized mainly fully hydrolysed PVA. In this chapter, targeting to weaker polymer-polymer interactions, a PVA matrix with 88% hydrolysis grade, was used for the preparation of nanocomposite films. Furthermore, due to the presence of metal cations in the clay lattice, increased interactions between clay platelets and acetoxy groups of the PVA are expected (Stathi et al. 2009), boosting the intercalation /exfoliation of the inorganic layers. To this end, a series of PVA/ MMT clay composites were prepared by solvent film casting method using water as solvent. The obtained nanocomposites were characterised by a variety of techniques including XRD, TEM, AFM, DCS, TGA, mechanical strength, oxygen and water permeability and water sorption. The developed films, due to the favorable polymer-particle interactions, revealed excellent dispersion of the clay particles in the polymer matrix and improved properties.

3. Synthesis of PVA/MMT nanocomposites

3.1 Materials and methods

Low viscosity, partially hydrolyzed atactic Poly(vinyl alcohol) Mowiol® 5-88 (Average molecular weight: 37000 g/mol - Sigma) was used for the preparation of the nanocomposites. Na-MMT (cationic exchange capacity of 80 meq/100g) was supplied by S&B Industrial Minerals S.A. The purity (in montmorillonite) of raw clay used in this study was about 76%.

The developed nanocomposite films were characterised by a variety of microscopic and macroscopic techniques. The dispersion of the clay platelets was investigated by XRD, AFM and TEM. XRD patterns were recorded on a Siemens XD-500 diffractometer using CuKα1 radiation source, while Electron Transmission images were obtained using a Jeol JEM 2011 TEM. In addition, the Surface morphology was examined by a Digital Instruments Nanoscope III atomic force microscope (AFM), using tapping mode.

The oxygen permeability experiments at variant %RH were performed on a PBI Dansensor OPT-5000 instrument, according to ASTM F2622-08 method. The samples, prior to their testing, were conditioned in oven at a temperature of 50 ± 2 °C for 48 h (ASTM D 618 – Procedure B).

The mechanical strength of the films was measured by means of a Thumler GmbH Tensile Tester Model (cell load 250N -PA 6110 Nordic Transducer), using specimens of 3 cm width and 6 cm length. Prior the testing, the samples were pre-equilibrated at constant relative humidity.
A Modulated DSC Model 2920 TA Instruments was used to measure the thermal properties of the films, while a SETARAM SETSYS Evolution 18 Analyser (RT-1750^{o}C) was applied for the Thermogravimetric analysis of the samples. Additionally, the optical clarity of the materials was studied by UV-Vis spectroscopy (Cary 100 Varian Inc. UV-Vis spectrophotometer). The average samples' thickness used for optical measurements was 50±0.02 μm.
Finally, the sorption isotherm experiments were carried out on a homemade gravimetric system, equipped with a CI Electronics Ltd® microbalance and a SS gas/vapour dosing unit. The mass changes, the vapor pressure and the cell temperature were continuously recorded by means of LabVIEW® software.

3.2 Preparation of the PVA/MMT films

A PVA solution in water (10 wt%) was produced (6 hours mixing at 90^{o}C) and used as stock solution. The samples were prepared by mixing MMT water suspensions with the polymer solutions in quantities that gave 5, 10 and 20 wt% clay loading on the final films, namely PVA/MMT05, PVA/MMT10 and PVA/MMT0 respectively. Initially, the mixture of polymer and MMT (100ml) was stirred for half hour at 80^{o}C and then sonicated for an extra half hour. The suspension (10 to 20 ml regarding the final film thickness) was poured in square (12x12 cm) polystyrene Petri dishes and left to dry slowly at 25^{o}C for about 15 days. The average thickness of the samples used for permeability and mechanical tests was 0.1 ± 0.02 mm

4. Results and discussion

4.1 Morphology of developed composites

4.1.1 Microscopic techniques

Transmission Electron Microscopy (TEM) was used to for the preliminary characterization of the nanocomposites formed, with the emphasis on the dispersion of inorganic layers in the polymer matrix. Typical TEM images are shown in Figure 3 (a), (b), (c) for the 20 wt % MMT sample (PVA/MMT20). TEM observations reveal the existence of silicate layers in the exfoliated state. Furthermore, some larger intercalated tactoids could also be identified.
In addition to TEM, Atomic force microscopy (AFM) was also applied for the determination of the clay dispersion in PVA matrix. Figure 3(d) shows the corresponding AFM image of the PVA/MMT20 film, in tapping mode. The presence of disc shaped objects of about 50-140 nm can be attributed to the clay particles, while the linear parts (of about 20 nm) may be related to the polymer chains. In addition to the organization, a specific orientation of clay platelets is clearly obvious, in a wide area of the sample (about 2 μm^2). Although these organized regions may not be representative of the whole sample, reveal that the increased polymer-clay interactions lead to formation of exfoliated and intercalated structures. The obtained results are in good agreement with TEM observations. Thus, AFM can be a good alternative to electron microscopy for the analysis of nanocomposites, without any limitations regarding the contrast and the resolution.

4.1.2 XRD patterns

Wide angle X-ray diffraction is probably the most indicative technique to investigate the interactions between the polymer and inorganic layers. The XRD patterns of MMT powder, pure PVA film and nanocomposite films prepared in this study are shown in Figure 4. The peak at $2\theta = 7^{o}$ can be attributed to the basal spacing (~12.6 Å) of the MMT, while the other peak (around 29^{o}) can be related to clay impurities. In addition, the peak at $2\theta = 19.4^{o}$ (d = 4.57 Å) be present in pure polymer, can be attributed to crystal reflections of PVA.

On the other hand, the observed increase in the basal spacing of PVA/MMT20 sample (around 27Å) reveals the formation of intercalated structures, due to the polymer chains in the clay galleries. This expansion of the clay's basal spacing is due to favorable interactions between the clay's surface and the polymer groups. It must be noted that intercalated regions are obtained at lower clay concentration than previous studies have reported (Strawhecker & Manias, 2000).

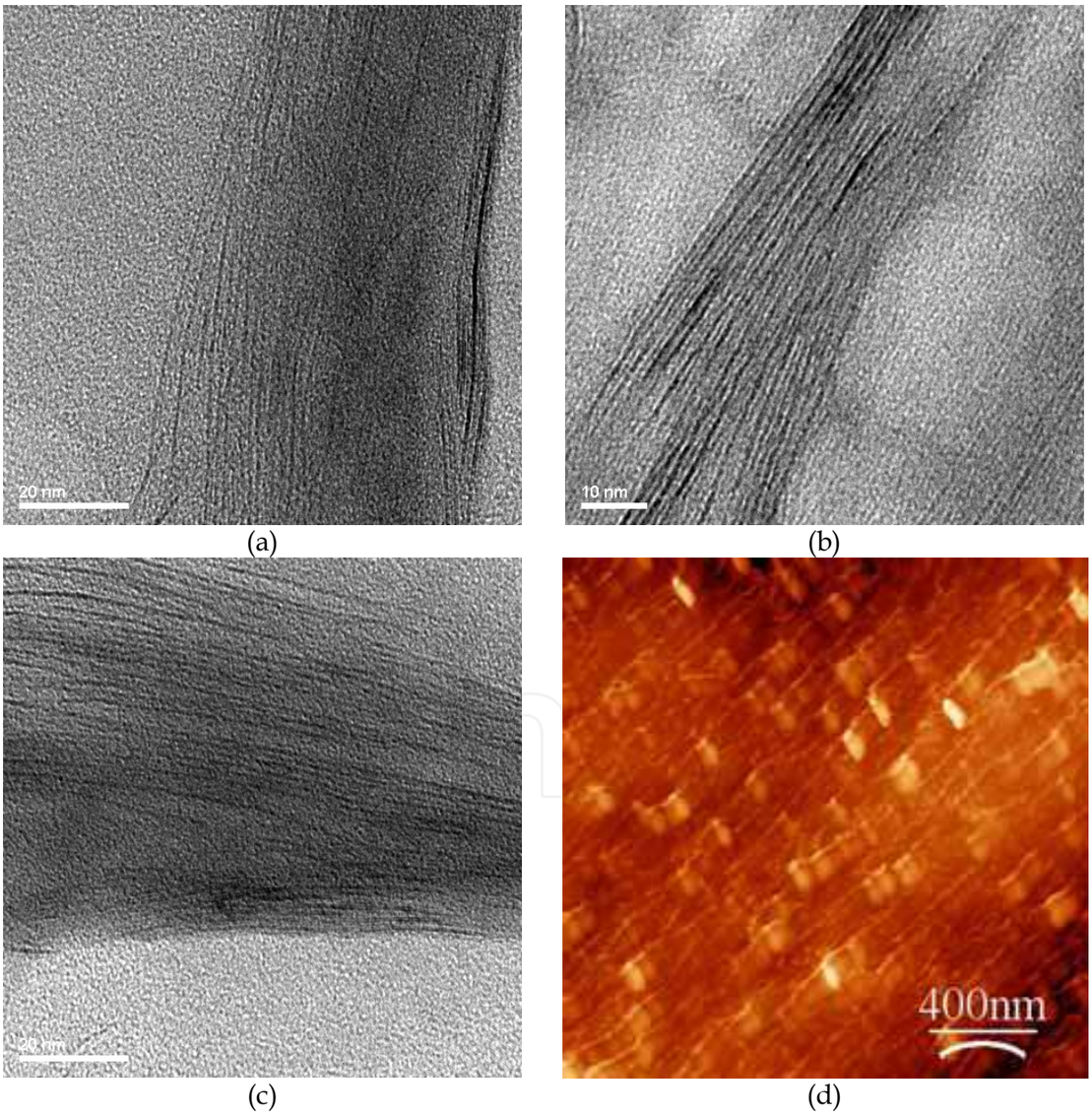

(a) (b) (c) (d)

Fig. 3. TEM micrographs (a), (b), (c) and AFM photo (d) of of PVA/MMT20 film

In the case of the PVA/MMT05 and PVA/MMT10 samples the peak corresponding to the basal distance is not apparent. Furthermore, the presence of a shoulder at clay's basal spacing reveals that a small part of the clay formed aggregates (Figure 4). Moreover, the increased background of these patterns suggests the existence of exfoliated inorganic layers in extended regions of the nanocomposite. These results are in agreement with the results obtained from the microscopic techniques.

In order to evaluate the orientation of the clay platelets, in regard to the film's surface, the following test was performed: the sample was measured in two forms, namely film and powder. The first time, the sample was left intact as a film and it was placed on top of the sample holder. The second time, the sample was fragmented into as small as possible pieces and measured again. The obtained patterns are shown in Figure 5. It is obvious that the peak corresponding to the basal spacing of the clay is less pronounced in the case of the powder sample, indicating that there is a specific orientation of clay particles, parallel to the surface of the nanocomposite film.

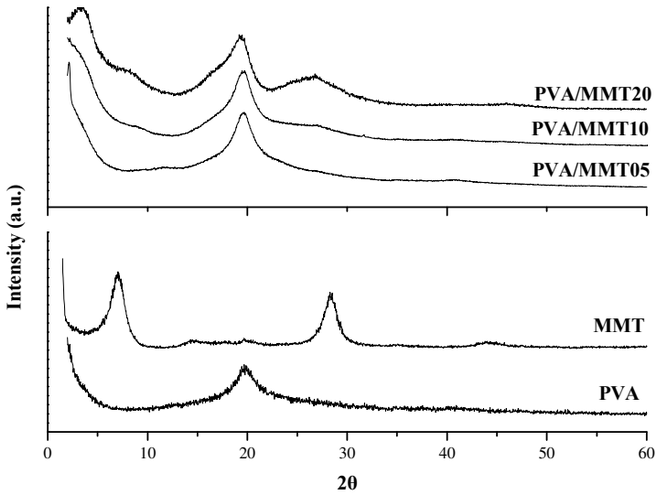

Fig. 4. XRD patterns of pure Montorillonite, PVA and Nanocomposite films

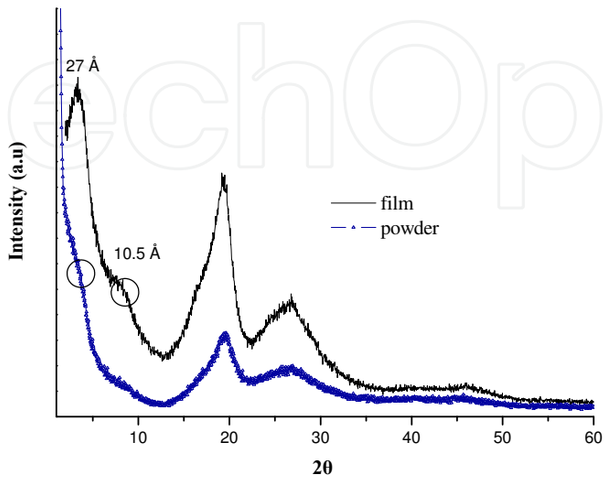

Fig. 5. XRD patterns of PVA/MMT20 sample powder and in film form

4.2 Gas permeability

Gas permeability is a very crucial property for various applications, including medical and industrial, which also apply to everyday materials, such as those used in packaging. The permeation of molecules through a non-porous polymeric membrane is determined by the capability of the molecules to be sorbed on the membrane's surface and body, to diffuse within and finally to be desorbed on the other side of the membrane.

The overall process is the product of the following coefficients:

a. Solubility (S) – the partition coefficient of sorbed, in regard to total molecules,
b. Diffusivity (D) - the rate of transport of molecules through the polymeric matrix.

The molecules' rate of transport through a polymer, as a result of the combined effects of diffusion and solubility, can be expressed by permeability coefficient (P_e), which is related to D and S by the expression:

$$P_e = D \times S \tag{2}$$

In this case, P_e incorporates both kinetic and thermodynamic properties of the polymer-permeant system.

The mass transport mechanism of gasses permeating a nano-platelet reinforced polymer is considered to be similar to that in a semicrystalline polymer. In most theoretical studies the nanocomposite is considered to consist of a permeable phase (polymer matrix), in which impermeable layers are dispersed (Cussler et al., 1998). The permeability of a nanocomposite system is mainly influenced by the following factors:

a. the volume fraction of the clay particles,
b. their orientation in relation to diffusion direction, and
c. the aspect ratio of the platelets.

It is generally accepted that the transport mechanism within the polymer matrix follows Fick's law, and that the matrix maintains the same properties and characteristics as the neat polymer. Thus, the diffusivity of the homogeneous matrix material D_0 is not influenced by the presence of particles. While this is likely a good assumption in many situations, certain exceptions are present in the literature, in which the anisotropic fillers in semicrystalline polymer matrices can influence the extent and morphology of crystalline regions, and thereby modify the matrix diffusivity.

Based on these assumptions, the tortuous path that is formed due to the presence of impermeable particles is analogous to the reduction of the diffusion coefficient (Figure 6). The tortuosity effect is related to the degree of the dispersion as well as to the aspect ratio of the layers and their orientation. Additionally, a decrease of the solubility is expected in the nanocomposite due to the reduced polymer matrix volume. Since the clay content in nanocomposites is usually small, the contribution of latter factor in overall permeability is less important.

Several models have been developed in order to predict the mass transfer through nanocomposites. A simple permeability model for a regular arrangement of platelets has been proposed by Nielsen (Nielsen, 1967):

$$\frac{P_e^{comp}}{P_e^{matrix}} = \frac{1-\varphi}{1+a/2\varphi} \tag{3}$$

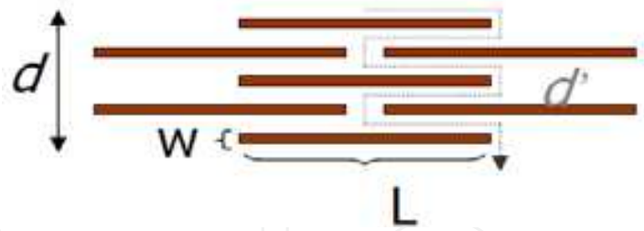

Fig. 6. Tortuous path according to Nielsen model

where P_e^{comp} and P_e^{matrix}, are the permeability coefficients for the composite and pure polymer film respectively, while

$$a = L/W \tag{4}$$

is the aspect ratio of the nanoplatelets and φ, the volume fraction of the clay into the composite. Although its simplicity, Nielsen model has been widely accepted and fits experimental observations well in several cases, especially for small volume fractions (below 10%) (Sun et al., 2008), (Wang et al., 2005)

Since the Nielsen model assumes more or less a perfect arrangement of the clay particles several other permeability models were based on the assumption of non-perfect alignment of platelets. A novel equation (Bharadwaj, 2001) introduces the parameter S, which is connected to the apparent mean angle, θ, of the platelet's long end and of the diffusion front by the following expression:

$$S = \frac{1}{2}(3\cos^2\theta - 1) \tag{5}$$

The reduction in the permeability of the nanocomposite can then be described by following equation:

$$\frac{P_e^{comp}}{P_e^{matrix}} = \frac{1-\varphi}{1+\frac{L}{2W}\varphi\left(\frac{2}{3}\right)\left(S+\frac{1}{2}\right)} \tag{6}$$

In the case that the platelets are randomly orientated (S=0), tortuosity decreases and diffusion is enhanced more, than in the case of vertically to the diffusion oriented platelets (S=1 reduces to Nielsen model). It should be noted that both the abovementioned models are based on the fact that diffusion is the dominant mechanism that determines the overall permeability.

Figure 7 presents the oxygen permeability at 23°C at different relative humidity values. A significant improvement of the gas barrier properties is observed for all studied samples. Thus, the permeability of the PVA/MMT20 at 50% RH decreases to almost 10% of the corresponding value of the pure PVA film. On the other hand, the permeability of the nanocomposites increases at higher %RH, although the obtained values are still much lower than the permeability of the pure PVA, at the same relative humidity. In this case, the water acts as plastisiser, facilitating the transport of oxygen molecules through the film.

The application of Nielsen model to the experimental data resulted in an aspect ratio (α) of ~70 in the case of 50% RH measurements. The calculated aspect ratio value is similar to that derived from AFM measurements. This implies that larger portion of the clay layers are delaminated within the polymer matrix.
At higher %RH, the predicted from Nielsen model aspect ratios decrease (to 20, 10 and finally to 2 for 65%, 75% and 85% RH respectively), revealing that the barrier effect of clays becomes less significant, as relative humidity increased. In these cases, the flow properties are mainly determined by the transport of the gas molecules though the swelled polymer.
It has also been reported that the presence of the inorganic platelets can affect the free volume of the polymeric phase, especially when there is low affinity between polymer and clay. In such a case, the permeability is determined by the counterbalance effects of reduction due to impermeable clay layers and the increase due to enhanced free volume (Incarnato et al., 2003).
In general, strong polymer–clay interactions can affect crystallinity, molecular orientation, and packing of the molecules near the nanoplatelets, leading to an enhancement in gas barrier properties, while poor adhesion between nanoplatelets and matrix usually results in opposite effect (Chaiko & Leyva, 2005), (Osman et al., 2003).

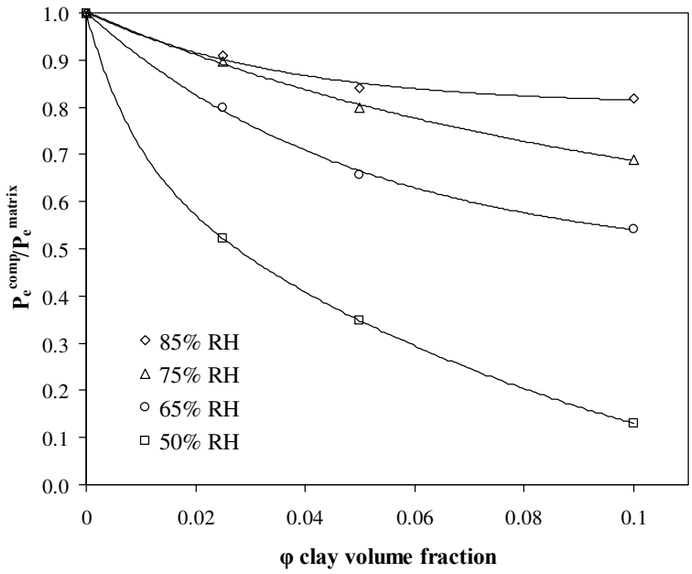

Fig. 7. Oxygen permeability of composite films presented in relation to pure PVA values

4.3 Mechanical properties

The clearest advantage of nanocomposites against conventional composite materials is the great improvement in their tensile properties, by small nanofiller addition. This result is caused mainly by the high surface area of the filler, which interact in the nanoscale with the matrix. The mechanical properties of polymers are influenced by many factors such as exposure to solvents, temperature, aging etc. Thus, it is of great importance to determine the mechanical properties under standard conditions.
In the case of the produced PVA/MMT nanocomposites, the measurements were performed at ambient humidity (~50% RH) and 23 ^{o}C, while the samples were pre-equilibrated at 45 and 70 %RH prior their testing. Figure 8 demonstrates the measurements for the Young's modulus and the elongation of the samples for 45% and 70% RH. In ambient humidity

conditions (45 %RH), Young's modulus value increases along with clay content increment, resulting to a maximum of 2.6 times for the case of PVA/MMT20 (in comparison with pure PVA). The great improvement in the Young modulus in PVA/MMT nanocomposites can be attributed to the strong interaction between matrix and silicate layers via formation of hydrogen bonds, due to the strong hydrophilicity of the clay edges (Sengwa, 2009).
At elevated RH (70%), the influence of the clay is much greater. Therefore, for the PVA/MMT05 sample the increase is more than 9 times and for PVA/MMT20 almost 193 times, respectively. The difference in the values, obtained between the two different relative humidity conditions, is due to the water's strong plasticization ability for PVA. Thus, while water can not influence the strength of clay particle, affects greatly the mechanical properties of PVA. Therefore, the effect of MMT on mechanical properties of the nanocomposites is more pronounce at higher %RH.

4.4 Thermal properties

An additional important aspect of nanocomposites is their increased heat resistance. The thermogravimetric curves of the samples are shown in Figure 9. The major weight losses are observed in the range of 200–500 ^{o}C, which corresponds to the structural decomposition of the PVA. Moreover, the nanocomposites exhibit significant less weight loss, in regard to pure PVA. Thus, for the PVA/MMT20 sample the weight loss at 400 ^{o}C is around 40% less of that for the neat polymer. It is also clear that the onset degradation temperature of the nanocomposites is slightly increased by the incorporation of the clay.

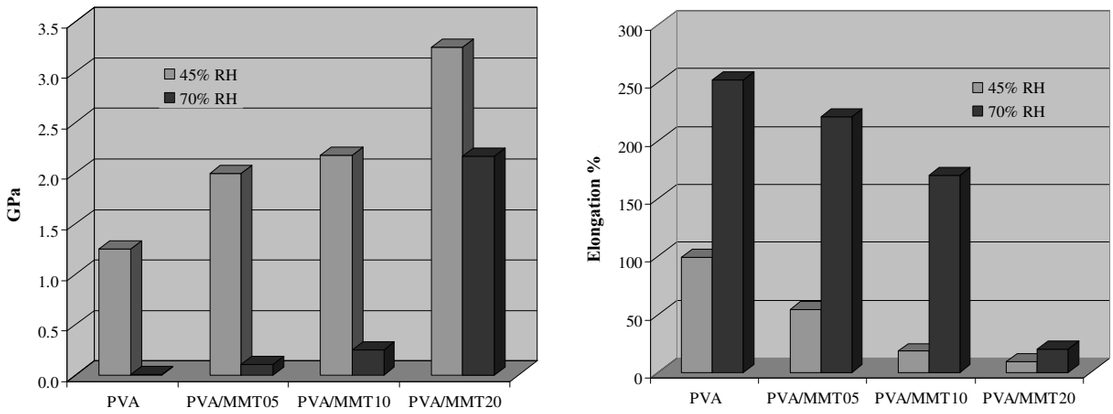

Fig. 8. Mechanical properties of developed nanocomposites (Left: Young Modulus, Right: Elongation values)

The enhancement in the thermal stability of the nanocomposites is due to the presence of clay nanolayers, which act as barriers to maximize the heat insulation and to minimize the permeability of volatile degradation products through the material (Chang et al., 2003).
Furthermore, DSC experiments reveal a decrease in crystallinity of the polymer with increasing clay content. Additionally, a second endothermic peak around 210 ^{o}C is observed (Figure 9 b), which can be attributed to the existence of a new crystal phase, induced by the presence of the clays. The enthalpy of fusion of this peak is linearly related to the clay content, suggesting that the inorganic layers are well dispersed, either intercalated or exfoliated, in the polymer. These results are in good agreement with the results obtained from the study of similar polymer-clay systems (Strawhecker & Manias, 2000).

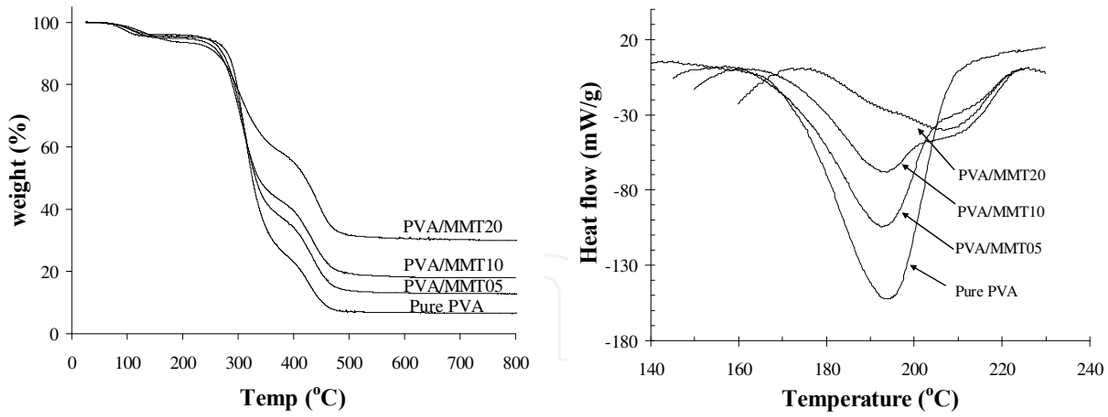

(a) (b)

Fig. 9. TGA (a) and DSC (b) curves of PVA/MMT naonocomposites

4.5 Optical properties

In general, the optical clarity of the nanocomposites can be related to the dispersion of the inorganic paltelets into polymer matrix: well dispersion in nanoscale will lead to exfoliated composites with high optical clarity. Reinforcing agents, in micrometer scale, usually scatter the light and thus reduce the light transmittance and the optical clarity of the composites. The same effect is observed when clay aggregates are formed. Due to their size (200-800 nm), clay aggregates cause strong scattering and/or absorption, resulting in very low transmission of the UV –Vis light. On the other hand, efficient dispersion in nanoscale, due to increased polymer- particle interfacial interactions, eliminates scattering and allows the preparation strong yet transparent films, coatings and membranes. The UV-Vis spectra of the prepared nanocomposites are shown in Figure 10. Contrary to previous studies (Yu et al., 2003) the prepared nanocomposite films retain the optical transparency of the pure PVA film in the visible region, even at high clay loading (up to 20% wt). This implies that the clay platelets are well dispersed in the PVA matrix.

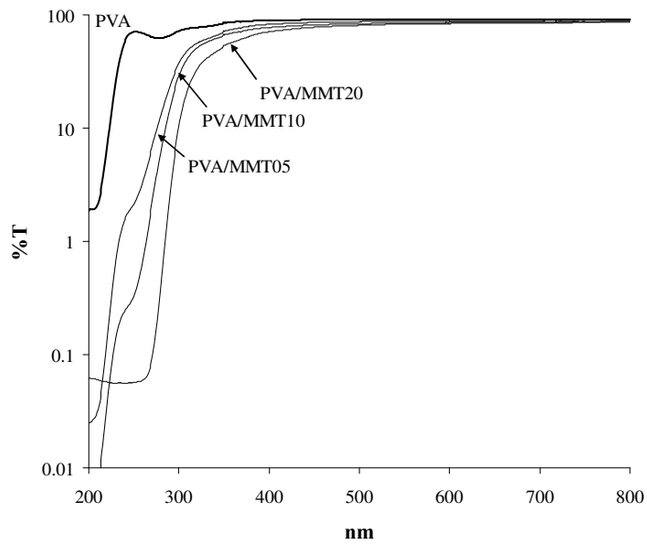

Fig. 10. UV-Vis spectra of developed nanocomposites films

4.6 Water sorption

The relationship between the concentration of water in a material at constant temperature and the water relative pressure (p/p_0) or water activity (a_w) is described by the water sorption isotherm.

The sorption isotherm can provide useful information concerning the sorption mode and the interactions involved in the sorption process. Several theoretical models have already been used to describe sigmoidal type isotherms. Models available in the literature to describe moisture sorption isotherm can be divided into several categories (Al-Muhtaseb et al., 2004): (a) models based on a monolayer adsorption (BET model), (b) models based on a multi-layer and condensed film (GAB model), (c) semi-empirical (Ferro-Fontan, Henderson and Halsey models) and (d) empirical models (Smith and Oswin models). In general, adsorption isotherms can be used for the determination of both the diffusion coefficient and the solubility and, therefore, the permeability of the films using Equation 2.

Sorption isotherm curves are obtained by plotting, the concentration of sorbed water (q^{Ads} in mg water/g sample) versus the water relative pressure (p/p_0). The sorption isotherms of pure PVA, MMT and PVA/MMT20 film are presented in Figure 11.

The shape of the nanocomposites water sorption isotherms is similar to that of the reference matrices, showing that the sorption mechanism is mainly governed by the same mechanism as in polymer matrix. In general, a sigmoidal shape corresponding to type IV sorption mode in the classification of Brunauer–Emmett–Teller is clearly observed for both films (Brunauer et al., 1940). This curve shape is typical for many hydrophilic materials (Gocho et al., 2000), (Masclaux et al., 2010).

At low water concentrations ($p/p0<0.4$) the behavior of nanocomposite film is almost identical to that of pure polymer. At higher relative pressures, an increase in both adsorption capacities is observed due to the enhanced molecular mobility of the polymer chains in the presence of water, which acts as plasticiser. Moreover, the sorbed amount for pure PVA film is much greater than the corresponding value of nanocomposite film.

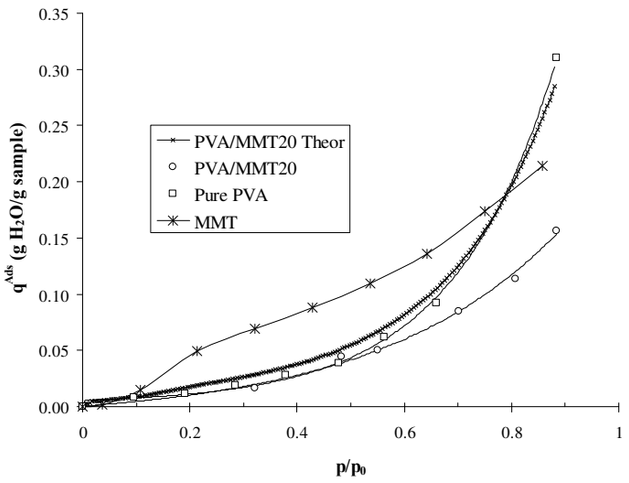

Fig. 11. Experimental water adsorption isotherms of pure PVA and PVA/MMT20 films and theoretical isotherm of PVA/MMT20 assuming no interactions between clay layers and polymer.

It should be noted that in the case of PVA/MMT20 the water uptake is lower than the calculated capacity, considering the contribution of each component, namely PVA and MMT, by means of an additive law, depending on their weight percentage (Figure 11). It

could then be concluded that some sorption sites in the polymer are not available for water sorption in the composite, probably due to their involvement in the formation of polymer/nanoclay interactions. This hypothesis is in good agreement with the results obtained by the other techniques, used in this study. Therefore, water sorption isotherms can be considered as a valuable technique for the characterization of nanocomposites, providing useful information not only about macroscopic characteristics of the materials such as solubility and the diffusivity coefficients, but also about the interfacial nanoscale phenomena occurring between polymer and inorganic layers.

5. Conclusions

A series of PVA/Montmorillonite nanocomposites were prepared by effective dispersion the inorganic platelets into PVA matrix, via solvent casting technique. The developed nanocomposites were studied by a variety of microscopic and macroscopic techniques. Morphological studies using TEM, proved the excellent dispersion of the clay particles into the polymer matrix and the formation of exfoliated and intercalated structures. These results were in agreement with the obtained XRD patterns. On the other hand, AFM revealed, apart from the organization, the specific orientation of the clay particles, parallel to the surface of the nanocomposite. Furthermore, the orientation of the MMT layers was also identified by combined diffraction experiments in film and in powder form.

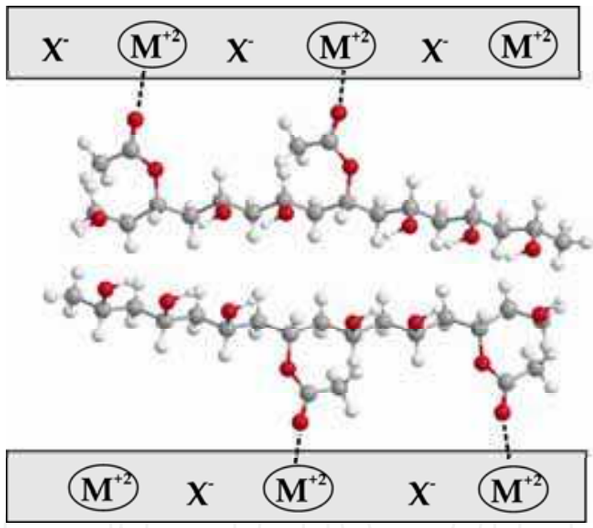

Fig. 12. Enhanced interactions between of partially hydrolised PVA and clay particles

The developed films, due to the favorable polymer-particle interactions, revealed excellent dispersion of the clay particles in the polymer matrix and improved mechanical strength, increased heat resistance and advanced gas barrier properties, retaining their optical transparency even at high clay loadings (20 wt %).

The application of the theoretical permeability model (Nielsen approximation) to the experimental data enabled the calculation of the theoretical aspect ratio of the clay (~70), which was in good agreement with the values obtained from the literature. This implied that the clay platelets were well-dispersed in the PVA matrix. Similar results were also obtained from water isotherm technique. In this case, the deviation of the experimental isotherm from the theoretical curve, calculated by the volume fraction additive law, revealed that a portion of the adsorption sites were used for the establishment of polymer-clay interactions.

Generally, the final properties of a nanocomposite are determined by the competitive effects of polymer-polymer and polymer-clay interactions. In PVA/MMT nanocomposites, the polymer –clay mixing can be settled by the interactions between the functional groups of PVA and the negative charge on clay surface. In our case, the acetoxy groups of the partially hydrolised PVA together with the presence of metal cations in the clay lattice, lead to the formation of strong polymer – clay interactions (Figure 12), promoting the dispersion of the inorganic layers into the polymer matrix. These interactions enabled the formation of intercalated and /or exfoliated structures, enhancing the overall material's performance.

6. References

Alexandre, M. & Dubois, P. (2000). Polymer-layered silicate nanocomposites: preparation, properties and uses of a new class of materials. *Materials Science and Engineering*, 28, 1-63

Al-Muhtaseb, A.H.; McMinn, W.A.M. & Magee, T.R.A. (2004). Water sorption isotherms of starch powders Part 1: mathematical description of experimental data. *Journal of Food Engineering*, 61, 297–307

Aranda, P. & Ruiz-Hitzky E. (1992). Poly(ethylene oxide)-silicate intercalation materials.' *Chemisty of Materials*, 4, 1395-403

Bafna, A.; Beaucage, G.; Mirabella, F. & Mehta, S. (2003). 3D Hierarchical orientation in polymer-clay nanocomposite films. *Polymer*, 44, 1103-15

Bharadwaj, R. (2001). Modeling the Barrier Properties of Polymer-Layered Silicate Nanocomposites. *Macromolecules*, 34, 9189-9192

Biswas, M. & Ray, S.S. (2001). Recent progress in synthesis and evaluation of polymer montmorillonite nanocomposites. *Advances in Polymer Science*, 155, 167-221

Brazel, C.S. & Peppas, N.A. (1999). Mechanisms of solute and drug transport in relaxing, swellable, hydrophilic glassy polymers. *Polymer,* 40, 3383-98

Brindley, G.W. (1984). In Crystal Structures and their X-Ray Identification, Mineralogical Society No.5, Brindley, G.W. & Brown, G., Eds, London, 169-172

Brunauer, S.; Deming, L.S. & Teller, E. (1940). On a theory of the van der Waals adsorption of gases. *Journal of the American Chemical Society*, 62, 1723–1732

Chaiko, D.J.; Leyva, A.A.(2005). Thermal transitions and barrier properties of olefinic nanocomposites. *Chemistry of Materials*, 17, 13–19

Chang, J.H.; Jang, T.G.; Ihn, K.J. & Sur G.S. (2003). Poly(vinyl alcohol) nanocomposites with different clays: pristine clays and organoclays. *Journal of Applied Polymer Science*, 90, 3204-14

Chin, I.-J.; Thurn-Albrecht, T.; Kim, H.-C.; Russell, T.P. & Wang, J. (2001). On exfoliation of montmorillonite in epoxy. *Polymer*, 42, 5947–52

Choudalakis, G. & Gotsis, A.D. (2009). Permeability of polymer/clay nanocomposites: A review. *European polymer Journa*l, 45, 967-984

Chuang, W.Y.; Young, T.H.; Chiu, W.Y. & Lin, C.Y. (2000). The effect of polymeric additives on the structure and permeability of poly(vinyl alcohol) asymmetric membranes. *Polymer*, 41, 5633-41

Clement, F.; Lapra, A.; Bokobza, L.; Monnerie, L. & P. Menez. (2001). Atomic force microscopy investigation of filled elastomers and comparison with transmission electron microscopy – application to silica-filled silicon elastomers. *Polymer,* 4, 6259–6270

Cussler, E.L.; Hughes, S.E.; Ward III, W.J. & Aris, R. (1988). Barrier Membranes. *Journal of Membranes Science*, 38, 161-174

Dennis, H.R.; Hunter, D.L.; Chang, D.; Kim, S.; White, J.L.; Cho, J.W. & Paul D.R. (2001). Effect of melt processing conditions on the extent of exfoliation in organoclay-based nanocomposites. *Polymer*, 42, 9513–22

Fischer, H. (2003). Polymer nanocomposites: from fundamental research to specific applications. *Materials Science and Engineering: C*, 23, 763–72.

Giannelis, E.P. (1996). Polymer Layered Silicate Nanocomposites. *Advanced Materials*, 8, 29-35

Giannelis, E.P. (1998). Polymer-Layered Silicate Nanocomposites: Synthesis, Properties and Applications. *Applied Organometallic Chemistry*, 12, 675-680

Giannelis, E.P.; Krishnamoorti, R. & Manias, E. (1999). Polymer-Silicate Nanocomposites: Model Systems for Confined Polymers and Polymer Brushes. *Advances in Polymer Science*, 138, 107-147

Gilman, J.W. (1999). Flammability and thermal stability studies of polymer layered-silicate (clay) nanocomposites. *Applied Clay Science,* 15, 31-49

Gilman, J.W.; Jackson, C.L.; Morgan, A.B.; Harris, R.; Manias, E.; Giannelis, E.P.; Wuthenow, M.; Hilton, D. & Phillips, H. (2000). Flammability Properties of Polymer−Layered-Silicate Nanocomposites. Polypropylene and Polystyrene Nanocomposites. *Chemistry of Materials*, 12, 1866-73

Gocho, H.; Shimizu, H.; Tanioka, A.; Chou, T.J. & Nakajima, T. (2000). Effect of polymer chain end on sorption isotherm of water by chitosan. *Carbohydrate Polymers*, 41, 87–90.

Greenland, D.J. (1963). Adsorption of poly(vinyl alcohols) by montmorillonite. *Journal of Colloid and Interface Science*, 18, 647-64

Grunlan, J.C.; Grigorian, A.; Hamilton, C.B. & Mehrabi, A.R. (2004). Effect of clay concentration on the oxygen permeability and optical properties of a modified poly(vinyl alcohol. *Journal of Applied Polymer Science,* 93, 1102- 109

Hay, J.M. & Lyon, D. (1967). Vinyl alcohol: a stable gas phase species. *Nature*, 216, 790–1.

Hernández, M.C.; Suárez, N.; Martínez, L.A.; Feijoo, J.L.; Mónaco, S.L. & Salazar, N. (2008). Effects of nanoscale dispersion in the dielectric properties of poly(vinyl alcohol)-bentonite nanocomposites. *Physical Review E*, 77, 051801

Herrmann, W.O. & Haehnel, W. (1924). *Germany Patents,* No. 480866

Hodge, R.M.; Bastow, T.J.; Edward, G.H.; Simon, G.P. & Hill A.J. (1996). Free Volume and the Mechanism of Plasticization in Water-Swollen Poly(vinyl alcohol). *Macromolecules*, 29, 8137-43

Incarnato, L.; Scarfato, P.; Russo, G.M.; Di Maio, L; Iannelli, P.; Acierno, D. (2003). Preparation and characterization of new melt compounded copolyamide nanocomposites. *Polymer* , 44, 4625–4634.

Jiang, T.; Wang, Y-H.; Yeh, J-T. & Fan, Z-Q. (2005). Study on solvent permeation resistance properties of nylon6/clay nanocomposite. European Polymer Journal, 41, 459-466

Katsaros, F.K.; Steriotis, Th.A.; Sapalidis, A.A. & Favvas, E.P. (2009). Neutron diffraction studies of polymer/Clay nanocomposites, in *BENSC Experimental Reports 2008*, A. Rodig, A. Brandt, H.A. Graf (Eds), page 212, Berlin

Kobayashi, M.; Toguchida, J. & Oka, M. (2003). Preliminary study of polyvinyl alcohol-hydrogel (PVA-H) artificial meniscus. *Biomaterials*, 24, 639-47.

Krishnamoorti, R.; Vaia, R.A. & Giannelis, E.P. (1996). Structure and dynamics of polymer-layered silicate nanocomposites. *Chemistry of Materials*, 8, 1728-1734

Lagaly, G. (1999). Introduction: from clay mineral-polymer interactions to clay mineral-polymer nanocomposites. *Applied Clay Science*, 15, 1-9

Lan, T.; Kaviratna, P.D.; Pinnavaia, T.J. (1994). On the nature of polyimide clay hybrid composites. *Chemistry of Materials*, 6, 573–575

LeBaron, P.C.; Wang, Z. & Pinnavaia, T.J. (1999). Polymer-layered silicate nanocomposites: an overview. *Applied Clay Science*, 15, 11–29

Lee, J.Y., Baljon, A.R.C.; Loring, R.F. & Panagiopoulos, A.Z. (1998). Simulation of polymer melt intercalation in layered nanocomposites., *Journal of Chemical Physics*, 109, 10321-30

Lee, S.S.; Hur, M.H.; Yang, H.; Lim, S. & Kim, J. (2006). Effect of interfacial attraction on intercalation in polymer/clay nanocomposites. *Journal of Applied Polymer Science*, 101, 2749-2753

Lim, Y.T. & Park, O.O. (2001). Phase morphology and rheological behavior of polymer/layered silicate nanocomposites. *Rheologica Acta*, 40, 220-229

Magonov, S.N. (2000). AFM analysis of polymers In: Encyclopedia of analytical chemistry, R.A. Meyers, (Ed), Wiley, Chichester, pp. 7432–7491, ISBN: 9783527293131

Magonov, S.N. & Reneker, D. (1997). Characterization of polymer surfaces with atomic force microscopy. *Annual Review of Materials Science*, 27, 175-222

Maiti, M. & Bhowmick, A.K. (2006). New insights into rubbereclay nanocomposites by AFM imaging. *Polymer*, 47, 6156-6166

Malwitz, M.M.; Dundigalla, A.; Ferreiro, V.; Butler,P.D.; Henk, M.C. & Schmidt, G. (2004). Layered structures of shear-oriented and multilayered PEO/silicate nanocomposite films. *Physical Chemistry Chemical Physics*, 6, 2977-2982

Masclaux, C.; Gouanvé, F. & Espuche, E. (2010). Experimental and modelling studies of transport in starch nanocomposite films as affected by relative humidity. *Journal of Membrane Science*, 363, 221–231

McNally, T.; Murphy, W.R.; Lew, C.Y.; Turner, R.J., & Brennan, G.P. (2003). Polyamide- 12 layered silicate nanocomposites by melt compounding. *Polymer*, 44, 2761–72

Messersmith, P.B. &, Giannelis E.P. (1995). Synthesis and barrier properties of poly(ε-caprolactone)-layered silicate nanocomposites. *Journal of Polymer Science Part A: Polymer Chemistry*, 33, 1047-57

Morgan, A.B. & Gilman, J.W. (2003). Characterization of poly-layered silicate (clay) nanocomposites by transmission electron microscopy and X-ray diffraction: a comparative study. *Journal of Applied Polymer Science*, 87, 1329-38

Morgan, A.B. (2006). Flame retarded polymer layered silicate nanocomposites: a review of commercial and open literature system. *Polymers for Advanced Technologies*, 17, 206-17

Nguyen, Q.T. & Baird, D.G. (2006). Preparation of Polymer–Clay Nanocomposites and Their Properties. *Advances in Polymer Technology*, 25, 270–285

Nielsen, L.E. (1967). Models for the Permeability of Filled Polymer Systems. *Journal of Macromolecular Science, Part A: Pure and Applied Chemistry*, 1, 929-941

Ogata, N.; Kawakage, S. &, Ogihara, T. (1997). Poly(vinyl alcohol)-clay and poly(ethylene oxide)-clay blend prepared using water as solvent. *Journal of Applied Polymer Science*, 66, 573-81

Osman, M.A.; Mittal, V.; Morbidelli, M.; Suter, U.W. (2003). Polyurethane adhesive nanocomposites as gas permeation barrier. *Macromolecules*, 36, 9851–9858

Osman, M.A.; Mittal, V.; Morbidelli, M.; Suter, U.W.(2004). Epoxy-layered silicate nanocomposites and their gas permeation properties. *Macromolecules*, 37, 7250–7257

Pavlidou, S & Papaspyrides, C.D. (2008). A review on polymer–layered silicate nanocomposites. *Progress in Polymer Science,* 33, 1119–1198

Pinnavaia, T. & Beall, G. (2000), Polymer-Clay Nanocomposites. Wiley: New York.

Podsiadlo, P.; Kaushik, A.K.; Arruda, E.M.; Waas, A.M.; Shim, B.S.; Xu, J.; Nandivada, H.; Pumplin, B.G.; Lahann, J.; Ramamoorthy, A. & Kotov, N.A. (2007). Ultrastrong and Stiff Layered Polymer Nanocomposites. *Science*, 318, 80-83

Ray S.S. & Okamoto, M. (2003). Polymer/layered silicate nanocomposites: a review from preparation to processing. *Progress in Polymer Science*, 28, 1539-641

Ray, S.S. & Bousmina, M. (2006). Biodegradable polymer/layered silicate nanocomposites, In: *Polymer nanocomposite,* Y-W. Mai & Z-Z. Yu (Ed.), 57-129, Woodhead Publishing Limited and CRC Press LLC, ISBN-13: 978-1-85573-969-7

Sapalidis, A.A.; Katsaros, F.K.; Romanos, G.E.; Kakizis, N.K. & Kanellopoulos, N.K. (2007). Preparation and characterization of novel poly-(vinyl alcohol)–Zostera flakes composites for packaging applications. *Composites Part B: Engineering*, 38, 398-404

Sengwa, R.J.; Choudhary, S.; Sankhla, S. (2009). Dielectric spectroscopy of hydrophilic polymers–montmorillonite clay nanocomposite aqueous colloidal suspension. *Colloids and Surfaces A: Physicochemical and Engineering Aspects*, 336, 79–87

Sinha-Ray, S.; Yamada, K.; Okamoto, M. & Ueda, K. (2002). Polylactide-Layered Silicate Nanocomposite: A Novel Biodegradable Material. *Nano Letters*, 2, 1093-1096

Stathi, P.; Papadas, I.T.; Enotiadis, A.; Gengler, R.Y.N.; Gournis, D.; Rudolf, P. & Deligiannakis, Y. (2009). Effects of Acetate on Cation Exchange Capacity of a Zn-Containing Montmorillonite: Physicochemical Significance and Metal Uptake. *Langmuir*, 25, 6825–6833

Strawhecker, K.E. & Manias, E. (2000). Structure and Properties of Poly(vinyl alcohol)/Na+ Montmorillonite Nanocomposites. *Chemistry of Materials*, 12, 2943-2949

Sun, L.; Boo, W-J.; Clearfield, A.; Sue, H-J.; Pham, H.Q. (2008). Barrier properties of model epoxy nanocomposites. *Journal of Membrane Science*, 318, 129–136

Vaia, R.A.; Jant, K.D.; Kramer, E.J. & Giannelis, E.P. (1996). Microstructural evaluation of melt-intercalated polymer-organically modified layered silicate nano- composites. *Chemistry of Materials*, 8, 2628-35

Vaia, R.A.; Price, G.; Ruth, P.N.; Nguyen, H.T. & Lichtenhan, J. (1999). Polymer/layered silicate nanocomposites as high performance ablative materials. *Applied Clay Science*, 15, 67-92

Van der Hart, D.L.; Asano, A. & Gilman, J.W. (2001). Solid-state NMR investigation of paramagnetic nylon-6 clay nanocomposites. 2. Measurement of clay dispersion, crystal stratification, and stability of organic modifiers. *Chemistry of Materials*, 13, 3796-3809

Varlot, K.; Reynaud, E.; Kloppfer, M.H.; Vigier. G. & Varlet, J. (2001). Clay–reinforced polyamide: preferential orientation of the montmorillonite sheets and the polyamide crystalline lamellae. *Journal of Polymer Science Part B: Polymer Physics*, 39, 1360–70.

Wang, Y.; Zhang, H.; Wu, Y.; Yang, J.; Zhang, L. (2005). Preparation and properties of natural rubber/rectorite nanocomposites. European Polymer Journal ,41, 2776–2783.

Xu, R.; Manias, E.; Snyder A.J. & Runt, J. (2001). New Biomedical Poly(urethane urea)−Layered Silicate Nanocomposites. *Macromolecules*, 34, 337-9

Yalcin, B. & Cakmak, M. (2004). The role of plasticizer on the exfoliation and dispersion and fracture behavior of clay particles in PVC matrix: a comprehensive morphological study. *Polymer*, 45, 6623-6638

Yeh, J.-M. & Chang, K.-C. (2008). Polymer/layered silicate nanocomposite anticorrosive coatings. *Journal of Industrial and Engineering Chemistry,* 14, 275–291

Yu, Y.H.; Lin, C.Y.; Yeh, J.M. & Li, W.H. (2003). Preparation and properties of poly(vinyl alcohol)-clay nanocomposite material. *Polymer*, 44, 3553-60.

Zanetti, M.; Lomakin, S. & Camino, G. (2000). Polymer layered silicate nanocomposites. *Macromolecular Materials and Engineering*, 279, 1-9

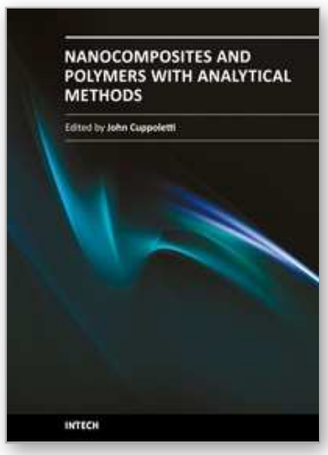

Nanocomposites and Polymers with Analytical Methods

Edited by Dr. John Cuppoletti

ISBN 978-953-307-352-1
Hard cover, 404 pages
Publisher InTech
Published online 09, August, 2011
Published in print edition August, 2011

This book contains 16 chapters. In the first part, there are 8 chapters describing new materials and analytic methods. These materials include chapters on gold nanoparticles and Sol-Gel metal oxides, nanocomposites with carbon nanotubes, methods of evaluation by depth sensing, and other methods. The second part contains 3 chapters featuring new materials with unique properties including optical non-linearities, new materials based on pulp fibers, and the properties of nano-filled polymers. The last part contains 5 chapters with applications of new materials for medical devices, anodes for lithium batteries, electroceramics, phase change materials and matrix active nanoparticles.

InTech Europe
University Campus STeP Ri
Slavka Krautzeka 83/A
51000 Rijeka, Croatia
Phone: +385 (51) 770 447
Fax: +385 (51) 686 166
www.intechopen.com

InTech China
Unit 405, Office Block, Hotel Equatorial Shanghai
No.65, Yan An Road (West), Shanghai, 200040, China
中国上海市延安西路65号上海国际贵都大饭店办公楼405单元
Phone: +86-21-62489820
Fax: +86-21-62489821

IntechOpen